JOURNAL OF CATALYSIS **162,** 277–283 (1996)
ARTICLE NO. 0285

# Influence of Hydrogen Chemisorption on the Surface Composition of Pt–Rh/$Al_2O_3$ Catalysts

N. Savargaonkar,*,† B. C. Khanra,‡ M. Pruski,† and T. S. King*,†,[1]

*Department of Chemical Engineering, Iowa State University, Ames, Iowa 50011-2230; †Ames Laboratory, Ames, Iowa 50011; and ‡Saha Institute of Nuclear Physics, Calcutta 700064, India

Received February 16, 1996; revised April 15, 1996; accepted April 16, 1996

**The surface compositions of a series of platinum–rhodium bimetallic catalysts supported on $\gamma$-alumina were determined in the presence of chemisorbed hydrogen by $^1$H NMR spectroscopy. The surface compositions of hydrogen-covered Pt–Rh bimetallic catalysts were found to be slightly enriched in Rh, significantly different from the surface compositions of adsorbate-free Pt–Rh surfaces, which are enriched in Pt. Further, based on selective excitation NMR experiments it was found that bimetallic particles of fairly uniform compositions were formed. Atomistic simulations of hydrogen-covered Pt–Rh bimetallic catalysts were done using a method that involved coordination-dependent bond energies. The simulations indicated that the heat of adsorption of hydrogen on rhodium is about 13 kJ/mol higher than that on platinum. Finally, a general, qualitative method for predicting the influence of adsorbates on the surface segregation behavior of bimetallic systems is described on the basis of knowledge of the surface energies at various sites and the heats of adsorption.** 

## INTRODUCTION

Supported bimetallic or multimetallic catalysts are commercially useful because they often exhibit improved activity, selectivity, or stability compared to monometallic catalysts (1). For example, platinum–rhodium catalysts find applications in industrially important reactions such as oxidation of ammonia to nitric oxide, control of automobile exhaust emission, and synthesis of hydrogen cyanide (2). In addition to their various applications, such catalysts offer opportunities to explore challenging scientific questions. In principle, one can vary the surface properties of these catalysts in a systematic manner simply by altering the overall metal composition (3–5). The composition of bimetallic catalysts is often significantly different at the surface compared to the bulk due to the differences in surface energies of the two metals. The surface composition or the relative fraction of the two metals at the surface is an important parameter in the study of catalytic phenomena. For example, the activity per metal site (turnover frequency) of reactions, which is needed to deduce the reaction mechanisms from kinetic data and to understand controlling factors such as ensemble or electronic effects, is based on the surface composition of the catalytically active metal (1, 6–8).

It is well known that adsorbates on bimetallic surfaces can alter the surface composition of such systems, and while various theoretical models (9–13) can predict the surface segregation behavior of a particular bimetallic system, the influence of adsorbates is difficult to quantify. In the case of the platinum–rhodium bimetallic system both theory and experiment (13–16) suggest that platinum segregates to the surface of a clean Pt–Rh bimetallic. Although the bulk cohesive energy of Rh is slightly smaller than that of Pt, the surface energy of Rh is larger than that of Pt. However, the difference in the surface energies of Pt and Rh is small and this difference can be altered by an adsorbate, perhaps even resulting in a reversal of the surface segregation behavior of the Pt–Rh system. For example, in the presence of oxygen it was observed using Auger electron spectroscopy (AES) and ion scattering spectroscopy (ISS) that the surfaces of Pt–Rh single crystals were enriched in Rh (17–20).

The influence of hydrogen on the surface composition of Pt–Rh bimetallic system has been studied less extensively. van Delft *et al.* (17, 18) studied Pt–Rh single crystals in the presence of hydrogen and other adsorbates using AES and reported that hydrogen did not influence the alloy as much as $O_2$ and NO, but quantitative information about the influence of $H_2$ was not given. Beck *et al.* (19, 20) using ISS and AES reported that the surface of a $Pt_{10}Rh_{90}$(111) single crystal became enriched in Pt under low-pressure ($10^{-6}$ Torr) and high-pressure (38 Torr) environments of hydrogen in the temperature range 500–600°C.

A few studies of supported Pt–Rh catalysts using techniques such as transmission electron microscopy (TEM) (21), isotopic exchange (22), and nuclear magnetic resonance (NMR) spectroscopy (23, 24) have been pursued. Wang and Schmidt (21) using TEM reported that the surface of silica-supported Pt–Rh catalysts became enriched in Rh by oxidation–reduction cycling. Wang *et al.* (23, 24)

[1] To whom correspondence should be addressed.



0021-9517/96 $18.00

used $^{13}C$ NMR of adsorbed CO and $^{195}Pt$ NMR to study Pt–Rh bimetallic clusters supported on $\eta$-alumina. The surface was found to be slightly enriched in rhodium in the presence of adsorbed CO.

In this study, we report the use of $^{1}H$ NMR spectroscopy to determine the surface compositions of $\gamma$-alumina-supported Pt–Rh catalysts in the presence of hydrogen. This approach is based on a method employed earlier by Wu *et al.* (3) to determine the surface compositions of silica-supported Ru–Cu bimetallic catalysts using $^{1}H$ NMR Knight shifts. The experimental results are compared with atomistic simulations in order to estimate the difference in the energy of adsorption of hydrogen on the two metals.

## METHODS

### *a. Catalyst Preparation*

One platinum and one rhodium catalyst, each with a metal loading of 3 wt% and supported on $\gamma$-alumina (Johnson Matthey, BET surface area of 100 $m^2/g$), were prepared by incipient wetness impregnation method using $H_2PtCl_6 \cdot 6H_2O$ and $Rh(NO_3)_3 \cdot 2H_2O$ (AESAR) as precursors. Appropriate amounts of the metal salts were dissolved in distilled water and about 1 g of the alumina support/ml of water was added to the solution. The resulting slurry was dried at room temperature for 20 h and then at 393 K for 8 h. Three Pt–Rh bimetallic catalysts with metal loadings of 3% Pt–1% Rh, 3% Pt–3% Rh, and 1% Pt–3% Rh were prepared in a similar manner via coimpregnation.

All of the catalysts were reduced in flowing hydrogen at 673 K and subsequently washed with hot, deionized water to remove residual chloride and other soluble impurities. The final reduction was carried out at 673 K in the NMR probe for 2 h, evacuating and replacing the hydrogen every 30 min. Selective hydrogen chemisorption was used to measure the dispersion of the monometallic as well as the bimetallic catalysts. The total adsorption isotherm and the isotherm for weakly bound hydrogen were measured at room temperature using hydrogen pressures in the range 20 to 50 Torr and then extrapolated to zero pressure to obtain the amount of strongly bound hydrogen adsorbed on the catalysts. An equilibration time of 10 min was used under each pressure and the catalysts were evacuated to $5 \times 10^{-6}$ Torr for 10 min before recording the adsorption isotherm for weakly bound hydrogen according to a method described by Uner *et al.* (25). The dispersions of the 3% Pt and 3% Rh catalysts were 38 and 51%, respectively. The dispersions of 3% Pt–1% Rh, 3% Pt–3% Rh, and 1% Pt–3% Rh catalysts were 25, 20, and 18%, respectively.

### *b. NMR Experiments*

The NMR experiments employed a home-built spectrometer with a proton resonance frequency of 250 MHz. The measurements were done using a home-built *in situ* NMR probe connected to a vacuum/dosing manifold, which allowed for an easy control of hydrogen pressure during the measurements. The L-shaped NMR sample tube was filled with the catalyst and then placed in the NMR probe, which was connected to a standard gas manifold via a flexible tubing. The sample was reduced *in situ* at 673 K and cooled to 573 K, evacuated overnight, and then cooled to 304 K. Hydrogen was then dosed onto the sample at 304 K and equilibrated for 10 min before the NMR spectra were recorded. All spectra were recorded with a dwell time of 5 $\mu$s, a repetition time of 0.5 s, and the number of scans varying from 3600 to 7200. Selective excitation experiments were done using a delays alternating with nutations for tailored excitation (DANTE) pulse sequence consisting of 30 short pulses (26). A pulse separation of 10 $\mu$s was chosen, resulting in a total duration of the DANTE sequence of 300 $\mu$s and a corresponding spectral excitation width of $\approx$3.3 kHz. The overall flip angle of the DANTE sequence was adjusted by varying the width of the short pulse while the rf amplitude remained constant. Following the DANTE sequence, a final 90° pulse was applied followed by the detection of the free induction decay.

### *c. Simulations*

Atomistic simulations employing coordination-dependent bond energies were used to determine the surface compositions of bimetallic systems as a function of particle size, temperature, compositions, and chemisorption energetics (9, 13, 27). The energy of the bimetallic system is given by

$$E = \sum N_i^A \varepsilon(A_i) + \sum N_i^B \varepsilon(B_i) + N_{AB}(\omega/z), \qquad [1]$$

where $\varepsilon(A_i)$ and $\varepsilon(B_i)$ are the energies contributed by atoms $A$ and $B$, respectively, to each of its nearest-neighbor bonds with coordination $i$, $N_i^A$ and $N_i^B$ are the number of atoms of type $A$ and $B$, respectively, in each site, $N_{AB}$ is the number of $A$–$B$ bonds in the system, $\omega$ is the mixing or interchange energy between the unlike atoms, $A$ and $B$, and $z$ is the bulk coordination ($z = 12$ for *fcc* metals). The partial bond energies $\varepsilon(A_i)$ and $\varepsilon(B_i)$ are obtained either from the corrected effective medium theory or experimentally determined parameters (27). The surface energies at various surface sites for Pt and Rh can be calculated from these partial bond energies and are listed in Table 1 along with the interchange energy for the Pt–Rh system. In order to model chemisorption, a term corresponding to the difference between the energy of adsorption of the adsorbate on the two metals is added to the above expression [1] for the total energy of the system. We define this difference $\Delta$ for the Pt–Rh system as

$$\Delta = |\Delta H_{\text{ads, Rh}}| - |\Delta H_{\text{ads, Pt}}|, \qquad [2]$$

where $\Delta H_{\text{ads, Rh}}$ and $\Delta H_{\text{ads, Pt}}$ are the heats of adsorption of hydrogen on rhodium and platinum, respectively. The

**TABLE 1**

**Surface Energies (in kJ/mol) at Specific Surface Sites (27)**

| Site type | Formula for site energy $E$ | Surface fraction of site ($D = 31\%$) | $E_{Rh}$ | $E_{Pt}$ | $E_{Rh}$–$E_{Pt}$ |
|---|---|---|---|---|---|
| Bulk | $12\varepsilon_{12}$ | | −554.55 | −563.23 | |
| (111) plane | $9\varepsilon_9$–$12\varepsilon_{12}$ | 0.65 | 110.91 | 100.30 | 10.61 |
| (100) plane | $8\varepsilon_8$–$12\varepsilon_{12}$ | 0.13 | 148.52 | 139.84 | 8.68 |
| Edge | $7\varepsilon_7$–$12\varepsilon_{12}$ | 0.19 | 186.14 | 178.42 | 7.72 |
| Corner | $6\varepsilon_6$–$12\varepsilon_{12}$ | 0.03 | 224.71 | 217.96 | 6.75 |

*Note.* Mixing energy for Pt–Rh system is −0.67 kJ/mol.

values reported (28–30) for the heats of adsorption of hydrogen on Pt and Rh cover a wide range (see Table 2). Hence the simulations were pursued for a range of Δ values at 304 K and a value giving the best fit for experimental data was found.

## RESULTS

All the $^1$H NMR spectra obtained in this work exhibit a peak close to 0 ppm (from TMS), which represents diamagnetic hydrogen in the support, mainly due to hydroxyl groups. The hydrogen interacting with the conduction electrons of the metal particles appears as a second peak and is located significantly upfield.

The spectra in Fig. 1 were obtained for the 3% Rh/$Al_2O_3$ catalyst. The upfield peak at −135 ppm in Fig. 1a corresponds to hydrogen adsorbed on metallic particles of rhodium at 7 Torr and the spectrum in Fig. 1b was obtained after subsequent evacuation of the catalyst for 10 min. These shifts are consistent with previous studies. Sheng and Gay (31) reported shifts in the range of −140 to

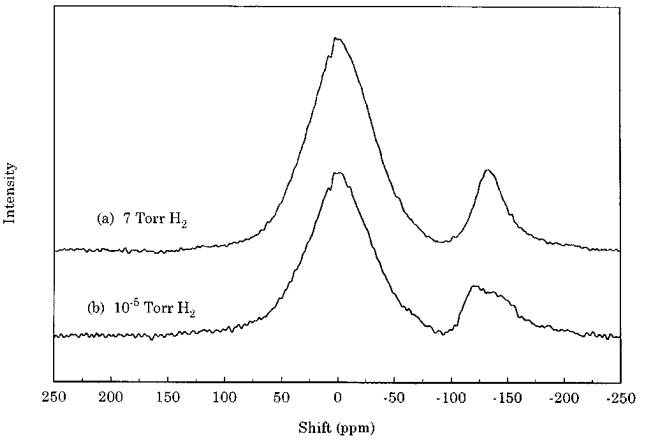


**FIG. 1.** $^1$H NMR spectra for 3% Rh/$\gamma$-$Al_2O_3$ catalyst with (a) 7 Torr $H_2$ and (b)$10^{-5}$ Torr $H_2$ after evacuation of $H_2$ in (a) for 10 min.

−170 ppm for hydrogen coverages varying from 0.3 to 1.0 on a 50% dispersed Rh/$SiO_2$ catalyst. Sanz and Rojo (32) observed a Knight shift of −120 ppm on Rh/$TiO_2$ catalysts at 10 Torr $H_2$.

The spectra for the 3% Pt supported on deuterated $Al_2O_3$ are shown in Fig. 2. The hydrogen-on-platinum (H/Pt) resonance shift is less than that for rhodium and strongly overlaps with the resonance from hydrogen in the support (Fig. 3a). In order to better resolve the H/Pt resonance, the support was subjected to deuterium exchange by heating to 673 K in 760 Torr of $D_2$ for 2 h, with fresh $D_2$ gas introduced at intervals of 30 min. The sample was then evacuated to $10^{-6}$ Torr and cooled to room temperature. The $^1$H NMR spectrum of the deuterated support (Fig. 2a) indicated a greatly diminished proton intensity near 0 ppm. Subsequently, hydrogen gas was introduced at an equilibrium pressure of 7 Torr (Fig. 2b). Hydrogen adsorbed on

**TABLE 2**

**Heats of Adsorption of Hydrogen on Pt and Rh in Various Forms**

| Metal | Form | Temperature range (K) | $\Delta H_{ads,H2}$ (kJ/mol) | Technique | Ref. |
|---|---|---|---|---|---|
| Pt | Film | 278–395 | 33–87 | Thermal desorption | (30) |
| | Foil | 140–600 | 67 | Thermal desorption | (30) |
| | Filament | 300 | 108 | Thermal desorption | (30) |
| | Tip | 4.2–300 | 67 | Field emission | (30) |
| | Tip | 83–293 | 62 | Work function | (30) |
| | Tip | 80–300 | 105.2 | Work function | (29) |
| | Supported: | | | | |
| | (i) Charcoal | | 97–109 | Calorimetry | (28) |
| | (ii) $\eta$-$Al_2O_3$ | 723 | 49 | Calorimetry | (28) |
| | (iii) $SiO_2$-$Al_2O_3$ | 723 | 46 | Calorimetry | (28) |
| | (iv) $SiO_2$ | 673–723 | 83–110 | Calorimetry | (28) |
| | (v) $TiO_2$ | 473–773 | 25–97 | Calorimetry | (28) |
| Rh | Film | Room temp. | 117.1 | Calorimetry | (30) |
| | Filament | 100–300 | 75.3 | Thermal desorption | (30) |
| | Filament | 196–350 | 79.4 | Field emission | (29) |

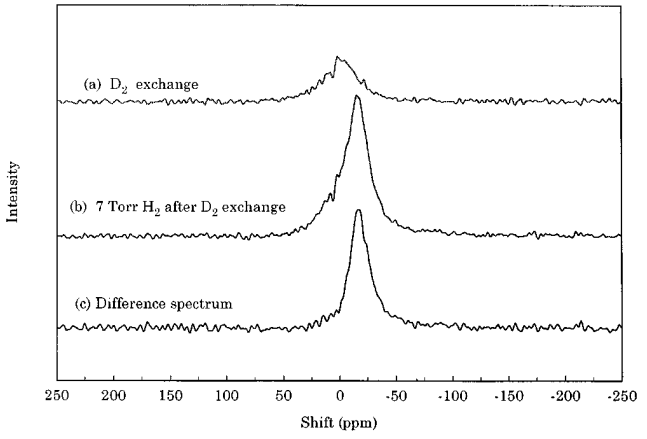


**FIG. 2.** $^1$H NMR spectra for 3% $Pt/Al_2O_3$ catalyst with deuterium exchanged with support hydrogen at 397°C for 2 h, (a) evacuated to $5 \times 10^{-6}$ Torr, (b) same sample in (a) with 7 Torr $H_2$, (c) difference spectrum of (b)–(a).

Pt is represented by the difference of these two spectra (Fig. 2c) and exhibits a relatively narrow peak at −16 ppm. This result is consistent with earlier work by Sheng and Gay (31, 33) who reported $^1$H NMR shifts in the range −50 to −20 ppm for Pt particles with hydrogen coverage varying from 0.2 to 1.0 on a $Pt/SiO_2$ catalyst with a dispersion of 30% and of about −10 ppm for Pt particles with hydrogen coverage of 1.0 on a 40% dispersed $Pt/Al_2O_3$ catalyst.

The results for the monometallic Pt and Rh catalysts are compared with the bimetallic Pt–Rh catalysts in Fig. 3. All spectra were taken after exposure to hydrogen at 7 Torr for about 10 min and show an increasing upfield shift of the hydrogen-on-metal resonance with increasing Rh content. The values of Knight shifts for hydrogen interacting with metallic particles in these spectra are given in Table 3.

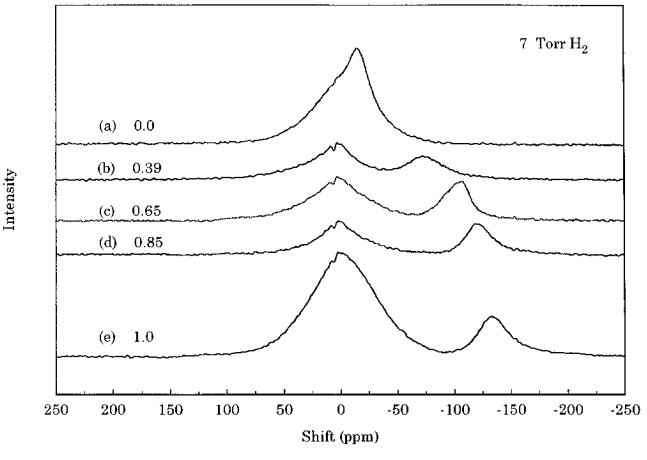


**FIG. 3.** $^1$H NMR spectra of hydrogen chemisorbed on the monometallic Pt and Rh and three bimetallic Pt–Rh catalysts supported on $\gamma$-$Al_2O_3$ with 7 Torr of hydrogen. (a) 3% Pt, (b) 3% Pt–1% Rh, (c) 3% Pt–3% Rh, (d) 1% Pt–3% Rh, and (e) 3% Rh. The overall mole fraction of rhodium–$X^{O}_{Rh}$ is indicated for each catalyst.

**TABLE 3**

**$^1$H NMR Results of Hydrogen Chemisorbed on $\gamma$-$Al_2O_3$-Supported Catalysts**

| Catalyst | Knight shift $\delta$ (ppm) | Overall atom fraction, $X^{O}_{Rh}$ | Surface atom fraction, $X^{S}_{Rh}$ |
|---|---|---|---|
| 3% Pt | −16 | 0.0 | 0.0 |
| 3% Pt–1% Rh | −74 | 0.39 | 0.49 |
| 3% Pt–3% Rh | −110 | 0.66 | 0.79 |
| 1% Pt–3% Rh | −123 | 0.85 | 0.90 |
| 3% Rh | −135 | 1.0 | 1.0 |

*Note.* Errors in Knight shifts: ±1 ppm.

The spectra in Figs. 4a and 4b correspond to the 1% Pt–3% $Rh/Al_2O_3$ catalyst at 7 Torr $H_2$ and $10^{-5}$ Torr $H_2$ (after 10 min evacuation), respectively. The result of the selective excitation (DANTE) experiment with the 1% Pt–3% Rh catalyst is given in Fig. 5. It can be seen that the H/Pt–Rh resonance line was saturated at a pressure of 7 Torr (Fig. 5a). However, selective inversion of the population in the frequency band corresponding to the pulse sequence applied could be achieved at $10^{-5}$ Torr (Fig. 5b). The purpose of the selective excitation experiment was to verify the formation of bimetallic particles (explained in detail in the next section).

## DISCUSSION

It is first noted that only one upfield peak is observed in the spectra for all catalysts that were exposed to 7 Torr of hydrogen (see Fig. 3). Further, the hydrogen-on-metal peak shifts toward upfield as the Rh content increases. These observations allow us to utilize $^1$H NMR as a probe of the composition of bimetallic particles. To validate this method, we briefly summarize some of our earlier investigations of the dynamics of hydrogen on the surfaces of supported metals.

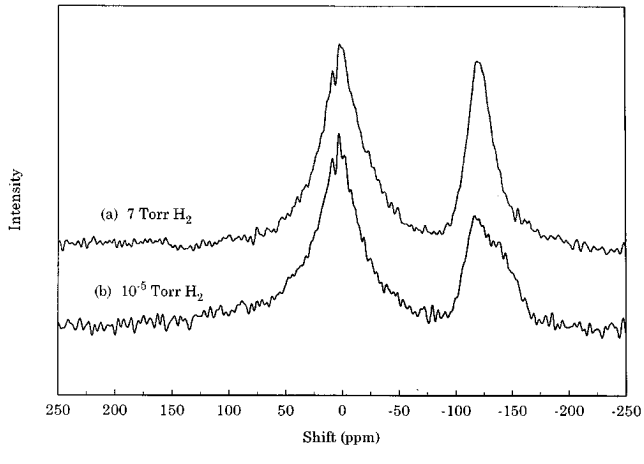


**FIG. 4.** $^1$H NMR spectra for 1% Pt–3% $Rh/Al_2O_3$ catalyst with (a) 7 Torr $H_2$ and (b) $10^{-5}$ Torr $H_2$ after evacuation of $H_2$ in (a) for 10 min.

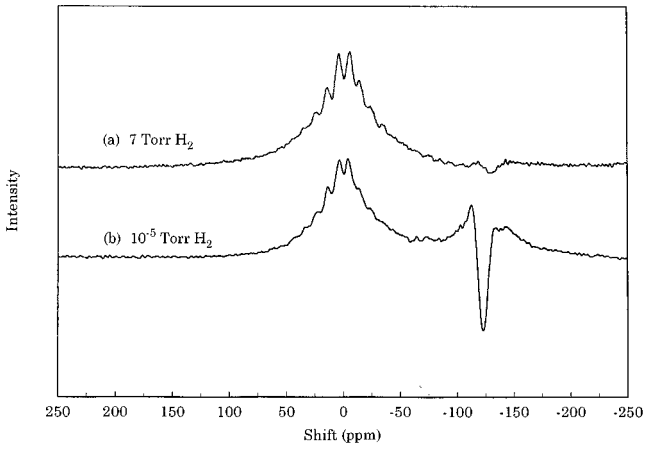


**FIG. 5.** $^1$H NMR selective excitation experiments for 1% Pt–3% Rh/$Al_2O_3$ catalyst with (a) 7 Torr $H_2$ and (b) $10^{-5}$ Torr $H_2$.

In a study of hydrogen adsorbed on silica-supported ruthenium, Engelke *et al.* (26) showed via selective excitation using the DANTE sequence that at low hydrogen pressures (e.g., $10^{-4}$ Torr) the hydrogen-on-metal NMR line is inhomogeneously broadened. It was also shown that the distribution of resonance frequencies resulted from differences in Knight shifts on particles of various sizes and shapes and not from heterogeneity of individual adsorption sites. Furthermore, under low pressures, the hydrogen may undergo a quasi-three-dimensional motion around the metal particles without desorbing from the surface. When the hydrogen pressure was increased to about 0.5 Torr, a transition from inhomogeneous to homogeneous line broadening occurred. A detailed analysis of lineshapes and the activation energies involved showed that this transition was a result of hydrogen motion that involved several processes: fast diffusion on a single particle, recombination, desorption, interparticle diffusion, and readsorption (26). A similar effect was observed when the selective excitation experiment was performed with the catalysts studied in this work: Under low hydrogen pressure of $10^{-5}$ Torr the line was inhomogeneously broadened, but a transition to homogeneous broadening occurred under elevated pressures. An example of such a transition is shown in Fig. 5 for a 1% Pt–3% Rh/$Al_2O_3$ catalyst. Thus, at a pressure of 7 Torr, hydrogen is in fast exchange with all surface metal sites present in the sample as it moves from one metal particle to another, whereas at $10^{-5}$ Torr the interparticle motion is restricted. Clearly, if monometallic Pt and Rh particles were present in large concentrations then two separate resonances corresponding to H/Pt and H/Rh would be visible under these lower pressures. Instead, only one resonance was observed at $10^{-5}$ Torr, which has a slightly increased linewidth and almost the same position compared to the resonance at 7 Torr (Fig. 4). This result suggests that for the most part bimetallic particles are formed and the concentration of monometallic particles is negligible. In addition, since the resonance at $10^{-5}$ Torr does not cover a broad range of resonances between H/Pt (−16 ppm) and H/Rh (−135 ppm), we can infer that the distribution of particle compositions is fairly narrow.

The interpretation of the observed shifts in terms of surface composition is not straightforward. It is generally recognized that the large $^1$H Knight shifts occur because of the bonding overlap between the hydrogen 1*s* orbitals and the conduction electrons of the underlying metals. Although the local density of electronic states on the surface of a bimetallic particle must reflect the surface segregation, it is not apparent at what range Pt and Rh retain their own electronic character. Two limiting cases can be considered: (I) a localized model that would result in the hydrogen shift on Pt and Rh to be independent of other neighboring and underlying atoms and identical to that on pure metals, and (II) a nonlocal picture that assumes that the adsorbed hydrogen experiences an average environment dependent on the sample composition. These two cases are discussed below in more detail.

(**I**) According to the localized model, in the absence of motion we should observe two resonance shifts $\delta_{Pt}$ and $\delta_{Rh}$ consistent with hydrogen on pure Pt and Rh. The presence of one hydrogen-on-metal resonance suggests that hydrogen is in fast exchange on Pt and Rh adsorption sites relative to the NMR time scale. The correlation time, $\tau_{ex}$, for this dynamic exchange process must satisfy the condition $\tau_{ex} \ll (2\pi\Delta\nu)^{-1}$, where $\Delta\nu$ is the difference between the resonance frequencies of the exchanging spins. In this exchange process an adsorbed proton experiences a Knight shift interaction that is proportional to the hyperfine field contributed from Pt and Rh sites in the lattice (34) and the observed shift, $\delta_{Pt\text{-}Rh}$, can be expressed by

$$\delta_{Pt-Rh} = \delta_{Pt} X^S_{Pt} + \delta_{Rh} X^S_{Rh}, \qquad [3]$$

where $X^S_{Pt}$ and $X^S_{Rh}$ are the surface atomic fractions of Pt and Rh, respectively. The above expression can be used to determine the surface compositions of Pt–Rh/$Al_2O_3$ catalysts from the monometallic shifts, $\delta_{Pt}$ and $\delta_{Rh}$, from Fig. 3a and 3e, respectively. This procedure is based on two further assumptions:

(i) The hydrogen-to-metal stoichiometry at the surface is the same for both metals. This assumption appears to be well justified by the results of $^1$H NMR spin counting. The integrated intensities of hydrogen-on-metal peaks in the $^1$H NMR spectra at 7 Torr of hydrogen yielded approximately the same H/$Pt_{surface}$ and H/$Rh_{surface}$ ratios [1.2 (±0.2) and 1.1 (±0.2), respectively] for the Pt/$Al_2O_3$ and Rh/$Al_2O_3$ catalysts.

(ii) The shifts $\delta_{Pt}$ and $\delta_{Rh}$ are both independent of particle size. This is justified simply by noting that the distribution of shifts for Pt/$Al_2O_3$ and Rh/$Al_2O_3$ is small compared to the difference between the resonance line positions for these two catalysts.

(**II**) The segregation of atoms on the surface of highly disordered bimetallic systems has been successfully described by the tight-binding Hartree–Hamiltonian model to determine the electronic energy (35). According to this model, the local electronic density of states $\rho_\lambda(E)$ of the bimetallic system can be described in terms of the densities of states of individual components (Pt and Rh in our case) as:

$$\rho_\lambda(E) = \rho_{\lambda,\mathrm{Pt}} X_{\lambda,\mathrm{Pt}} + \rho_{\lambda,\mathrm{Rh}}(1 - X_{\lambda,\mathrm{Pt}}). \qquad [4]$$

The above relationship is valid for the bulk as well as for surface layers (subscript $\lambda$ denotes the coefficients for the $\lambda$th layer). On the other hand, the Knight shift is dominated by the Fermi contact term, which can be expressed as $K = \langle a \rangle \chi_P$, where $\langle a \rangle$ denotes the hyperfine coupling constant and $\chi_P$ is the Pauli susceptibility. Since Pauli susceptibility is directly proportional to the density of states at the Fermi surface, the Knight shift for a disordered system can be also expressed by an equation similar to [4]. Thus, regardless of hydrogen dynamics and without the assumptions (i) and (ii) discussed earlier for the localized case, the NMR shifts can be used to determine a nonlocal concentration $X_{\mathrm{Pt}}$. Although it is unclear how many underlying layers affect the adsorbed atom, the data presented here indicate slight rhodium segregation (as discussed later) in the region of the particle that is probed by $^1$H NMR. The nonlocal model has been earlier postulated for similar Pt–Rh bimetallic clusters based on $^{13}$C NMR studies of adsorbed CO (23, 24).

We finally note that regardless of which model is operable in the system under study, NMR provides us with a unique and valid insight because it probes the very properties of the metal surface that are responsible for their catalytic performance, at least in reactions determined by the adsorption characteristics of hydrogen. The influence of hydrogen on the surface compositions of Pt–Rh catalysts, as observed in this work, is discussed below.

The experimentally determined and simulated values of surface rhodium composition (expressed as atom fraction) are plotted against the overall rhodium composition in Fig. 6. The simulations were performed at 304 K with the parameter $\Delta$ fitted to give the best agreement with the surface compositions derived from NMR. The difference in the heats of adsorption of hydrogen on Rh relative to Pt was found to be 13 kJ/mol at 304 K. The simulations pursued at 673 K (not shown), the reduction temperature which is the highest temperature possible for equilibration of compositions, yielded a value of 15 kJ/mol for $\Delta$ indicating that this parameter is relatively insensitive to temperature.

The results presented in Fig. 6 clearly demonstrate the influence of adsorbates on the surface composition of a bimetallic catalyst. In the case of the adsorbate-free Pt–Rh system, the difference in the surface energies between the two metals determined from the site energies (see Table 1) for a 31% dispersed particle is about 10 kJ/mol favoring Pt

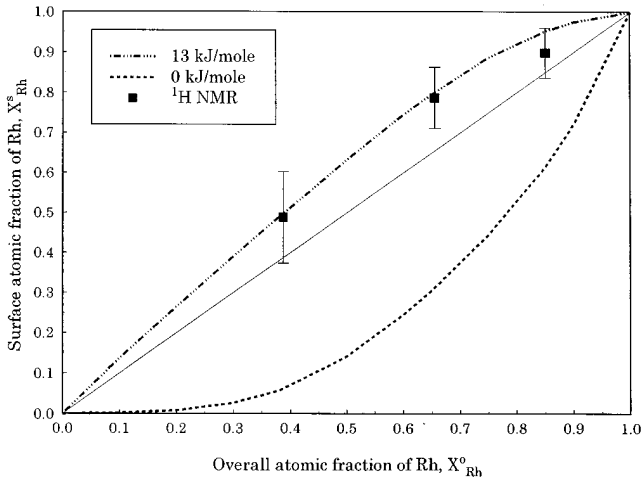


**FIG. 6.** Surface mole fraction of Rh against overall mole fraction of Rh for experimental data and atomistic simulations at 304 K in the presence and absence of hydrogen. The legend gives the values of $\Delta$ in kJ/mol, corresponding to the difference between the heats of adsorption of hydrogen on platinum and rhodium.

on the surface. In the presence of hydrogen, it is seen from experimental results and theory that the surface is slightly enriched in Rh with the heat of adsorption of hydrogen about 13 kJ/mol greater on Rh than on Pt.

The above qualitative analysis is a useful, general procedure to assess the potential for an adsorbate in a reactive environment to influence the surface composition of a bimetallic catalyst. An example where the surface composition is not influenced by hydrogen chemisorption is the Ru–Cu bimetallic system. The difference in surface energies between Ru and Cu for a closed packed surface as estimated from site energies is about 80 kJ/mol. The heats of adsorption of hydrogen on Ru and Cu are roughly 90 and 40 kJ/mol, respectively, and the corresponding difference of 50 kJ/mol is significantly smaller than the difference in the surface energies. Thus hydrogen cannot cause reversal of surface segregation behavior of the Ru–Cu bimetallic system and we would expect segregation of Cu to the surface of Ru–Cu bimetallic catalysts even in the presence of hydrogen. Indeed, Wu *et al.* (3), using $^1$H NMR, observed that copper segregated strongly to the surface of hydrogen covered Ru–Cu/$SiO_2$ catalysts.

## CONCLUSIONS

The surface compositions of Pt–Rh/$Al_2O_3$ catalysts in the presence of hydrogen were significantly different from those of adsorbate-free surfaces. The surface compositions determined via $^1$H NMR indicated that the surface was slightly enriched in Rh as opposed to enriched in Pt on an adsorbate-free surface. Furthermore, selective excitation NMR of adsorbed hydrogen indicated that these

Pt–Rh catalysts consisted primarily of bimetallic particles with a fairly narrow distribution of compositions.

A comparison of experimentally obtained surface compositions with simulated values gave an estimate of 13 kJ/mol for the difference between the heats of adsorption of hydrogen on Pt and Rh at 304 K with the heat of adsorption being higher on Rh. The approach given here can be generalized to predict the surface segregation behavior of a bimetallic system in the presence of various adsorbates if the overall difference between the metal surface energies and heats of adsorption of an adsorbate on the two metals are known. Such a method is very useful in predicting whether only one metal or both metals are present with significant concentration at the surface of bimetallic catalysts under reaction conditions. In this work, it was noted that both Pt and Rh were present in significant concentrations at the surface of Pt–Rh bimetallic catalysts under the influence of hydrogen adsorption. Quantification of surface compositions under reaction conditions gives useful information, which is needed to determine the catalytic activity per active metal site (turnover frequency). A better understanding of the catalytic activity of bimetallic systems can be gained if these results are correlated with reaction studies.

## ACKNOWLEDGMENTS

This work was supported by the U.S. Department of Energy, Office of Basic Energy Sciences, Division of Chemical Sciences, under Contract W-7405-ENG-82, and by the National Science Foundation, Engineering Research Equipment Grant CBT-8507418.

## REFERENCES

1. Sinfelt, J. H., "Bimetallic Catalysts" Wiley, New York, 1983.
2. Satterfield, C. N., "Heterogeneous Catalysis in Industrial Practice" McGraw-Hill, New York, 1991.
3. Wu, X., Gerstein, B. C., and King, T. S., *J. Catal.* **121**, 271 (1990).
4. Wu, X., Gerstein, B. C., and King, T. S., *J. Catal.* **123**, 43 (1990).
5. Bhatia, S., Engelke, F., Pruski, M., and King, T. S., *Catal. Today* **21**, 129 (1994).
6. Oliver, J. A., and Kemball, C., *Proc. R. Soc. London A* **429**, 17 (1990).
7. Goddard, S. A., Amiridis, M. D., Rekoske, J. E., Cardona-Martinez, N., and Dumesic, J. A., *J. Catal.* **117**, 155 (1989).
8. Wong, T. C., Chang, L. C., Haller, G. L., Oliver, J. A., Scaife, N. R., and Kemball, C., *J. Catal.* **87**, 389 (1984).
9. Strohl, J. K., and King, T. S., *J. Catal.* **116**, 540 (1989).
10. Burton, J. J., Hyman, E., and Fedak, D. G., *J. Catal.* **37**, 106 (1975).
11. Tsai, N., Abraham, F. F., and Pound, G. M., *Surf. Sci.* **77**, 465 (1978).
12. Sundaram, V. S., and Wynblatt, P., *Surf. Sci.* **52**, 569 (1975).
13. Schoeb, A. M., Raeker, T. J., Yang, L., Wu, X., King, T. S., DePristo, A. E., *Surf. Sci.* **278**, L125 (1992).
14. Williams, F. L., Nelson, G. C., *Appl. Surf. Sci.* **3**, 409 (1979).
15. Holloway, P. H., and Williams, F. L., *Appl. Surf. Sci.* **3**, 409 (1979).
16. van Langeveld, A. D., and Niemantsverdriet, J. W., *Surf. Sci.* **10**, 1 (1982).
17. van Delft, F. C. M. J. M., Nieuwenhuys, B. E., Siera, J., and Wolf, R. M., *ISIJ Int.* **29**(7), 550 (1989).
18. van Delft, F. C. M. J. M., Siera, J., and Nieuwenhuys, B. E., *Surf. Sci.* **208**, 365 (1989).
19. Beck, D. D., DiMaggio, C. L., Fisher, G. B., *Surf. Sci.* **297**, 293 (1993).
20. Beck, D. D., DiMaggio, C. L., Fisher, G. B., *Surf. Sci.* **297**, 303 (1993).
21. Wang, T., Schmidt, L. D., *J. Catal.* **71**, 411 (1981).
22. Kacimi, S., and Duprez, D., *Stud. Surf. Sci. Catal.* **71**, 581 (1991).
23. Wang, Z., Ph.D. thesis, Dept. of Physics, Univ. of Illinois at Urbana Champaign, 1987.
24. Wang, Z., Ansermet, J.-P., Slichter, C. P., and Sinfelt, J. H., *J. Chem. Soc. Faraday Trans. 1* **84**(11), 3785 (1988).
25. Uner, D. O., Pruski, M., and King, T. S., *J. Catal.* **156**, 60 (1995).
26. Engelke, F., Vincent, R., King, T. S., and Pruski, M., *J. Chem. Phys.* **101**(9), 7262 (1994).
27. Yang, L., and DePristo, A. E., *J. Catal.* **148**, 575 (1994).
28. Cardona-Martinez, N., and Dumesic, J. A., *Adv. Catal.* **38**, 149 (1992).
29. Gorodetskii, V. V., Nieuwenhuys, B. E., Sachtler, W. M. H., and Boreskov, G. K., *Surf. Sci.* **108**, 225 (1981).
30. Toyoshima, I., and Somorjai, G. A., *Catal. Rev.-Sci. Eng.* **19**(1), 105 (1979).
31. Sheng, T. C., and Gay, I. D., *J. Catal.* **77**, 53 (1982).
32. Sanz, J., and Rojo, J. M., *J. Phys. Chem.* **89**, 4974 (1985).
33. Sheng, T. C., and Gay, I. D., *J. Catal.* **71**, 119 (1981).
34. Khanra, B. C., and King, T. S., *Solid State Commun.* **89**, 269 (1994).
35. Mukherjee, S., Moran-Lopez, J. L., Kumar, V., and Bennemann, K. H., *Phys. Rev. B* **25**, 790 (1982).